Functional Transform-Based Low-Rank Tensor Factorization for Multi-Dimensional Data Recovery

Jianli Wang[1] and Xile Zhao[2]

[1] Southwest Jiaotong University, Chengdu, China
wangjianli_123@163.com
[2] University of Electronic Science and Technology of China, Chengdu, China
xlzhao122003@163.com

A Proof of Theorem 2

Proof. For any $i = 1, 2, \cdots, n_1$, $j = 1, 2, \cdots, n_2$, and $k = 1, 2, \cdots, n_3$, we have

$$\begin{aligned}
&\|\mathcal{X}(i,j,k) - \mathcal{X}(i,j,k-1)\|_{\ell_1}\\
=&\|((\mathcal{A} \triangle \mathcal{B}) \times_3 f_\theta(\mathbf{z}_{(k)}))(i,j) - ((\mathcal{A} \triangle \mathcal{B}) \times_3 f_\theta(\mathbf{z}_{(k-1)}))(i,j)\|_{\ell_1}\\
=&\|((\mathcal{A} \triangle \mathcal{B}) \times_3 (f_\theta(\mathbf{z}_{(k)}) - f_\theta(\mathbf{z}_{(k-1)})))(i,j)\|_{\ell_1}\\
\leq&\|\mathcal{A} \triangle \mathcal{B}\|_{\ell_1}\|f_\theta(\mathbf{z}_{(k)}) - f_\theta(\mathbf{z}_{(k-1)})\|_{\ell_1}\\
\leq&\|\mathcal{A}\|_{\ell_1}\|\mathcal{B}\|_{\ell_1}\|f_\theta(\mathbf{z}_{(k)}) - f_\theta(\mathbf{z}_{(k-1)})\|_{\ell_1}\\
\leq&\gamma_1\gamma_2\|f_\theta(\mathbf{z}_{(k)}) - f_\theta(\mathbf{z}_{(k-1)})\|_{\ell_1}.
\end{aligned}$$

Since $\sigma(\cdot)$ is Lipschitz continuous, thus, for any x, y, we have

$$\|\sigma(x) - \sigma(y)\|_{\ell_1} \leq \delta\|x - y\|_{\ell_1}.$$

Thus,

$$\begin{aligned}
&\|f_\theta(\mathbf{z}_{(k)}) - f_\theta(\mathbf{z}_{(k-1)})\|_{\ell_1}\\
=&\|\mathbf{H}_l(\sigma(\mathbf{H}_{l-1}\cdots\sigma(\mathbf{H}_1\mathbf{z}_{(k)}))) - \mathbf{H}_l(\sigma(\mathbf{H}_{l-1}\cdots\sigma(\mathbf{H}_1\mathbf{z}_{(k-1)})))\|_{\ell_1}\\
=&\|\mathbf{H}_l(\sigma(\mathbf{H}_{l-1}\cdots\sigma(\mathbf{H}_1\mathbf{z}_{(k)})) - \sigma(\mathbf{H}_{l-1}\cdots\sigma(\mathbf{H}_1\mathbf{z}_{(k-1)})))\|_{\ell_1}\\
\leq&\|\mathbf{H}_l\|_{\ell_1}\|\sigma(\mathbf{H}_{l-1}\cdots\sigma(\mathbf{H}_1\mathbf{z}_{(k)})) - \sigma(\mathbf{H}_{l-1}\cdots\sigma(\mathbf{H}_1\mathbf{z}_{(k-1)}))\|_{\ell_1}\\
\leq&\gamma_3\|\sigma(\mathbf{H}_{l-1}\cdots\sigma(\mathbf{H}_1\mathbf{z}_{(k)})) - \sigma(\mathbf{H}_{l-1}\cdots\sigma(\mathbf{H}_1\mathbf{z}_{(k-1)}))\|_{\ell_1}\\
\leq&\gamma_3\delta\|\mathbf{H}_{l-1}\cdots\sigma(\mathbf{H}_1\mathbf{z}_{(k)}) - \mathbf{H}_{l-1}\cdots\sigma(\mathbf{H}_1\mathbf{z}_{(k-1)})\|_{\ell_1}\\
&\cdots\\
\leq&\gamma_3^l\delta^{l-1}\|\mathbf{z}_{(k)} - \mathbf{z}_{(k-1)}\|_{\ell_1} = \frac{\gamma_3^l\delta^{l-1}}{n_3},
\end{aligned}$$

where $\{\mathbf{H}_i\}_{i=1}^l$ are the learnable weights of the MLP.
Combining the above inequalities, we have

$$\|\mathcal{X}(i,j,\mathbf{z}_{(k)}) - \mathcal{X}(i,j,\mathbf{z}_{(k-1)})\|_{\ell_1} \leq \frac{\gamma_1\gamma_2\gamma_3^l\delta^{l-1}}{n_3}.$$

The proof is complete.

B More Discussions

B.1 Comparison with HLRTF [1]

The proposed FLRTF itself can uniformly and harmonically capture the smoothness and low-rankness of data, however, HLRTF requires extra parametric total variation (PTV) regularization to capture the smoothness of data. Here, we give the comparison of the proposed FLRTF with HLRTF with PTV and without PTV. The results shown in Fig. 1 also demonstrate the superiority of the proposed FLRTF over HLRTF; more experiments see the manuscript.

HLRTF *wo* PTV	HLRTF with PTV	FLRTF	Ground truth
PSNR: 10.34 dB	PSNR: 38.24 dB	PSNR: 43.22 dB	PSNR: Inf

Fig. 1: The comparison of different methods.

B.2 Role of the Parameter r

The parameter r plays an important role for determining the degree of low-rankness. We conduct experiments to evaluate the effect of the parameter r on the performance of the proposed FLRTF. Fig. 2 illustrates the PSNR values corresponding to different parameter settings on MBI task. From Fig. 2, we can observe that when r is between 1 and 5, the PSNR value increases rapidly with the increase of r. The proposed FLRTF exhibits better performance when $r = 5$, and are stable as r increases. Based on this observation, we conclude that selecting $r = 5$ would be a suitable choice in our experiments.

B.3 Role of the Parameter $\hat{n}_3$

The parameter $\hat{n}_3$ controls the size of two latent factor tensors, which can be adjusted. Fig. 2 illustrates the PSNR values corresponding to different parameter settings on MBI task, where $\hat{n}_3$ takes the value kn_3 for $k = 1, 2, \cdots, 10$. We can observe that the PSNR value remains relatively stable overall, although there are minor fluctuations. Based on this observation, we conclude that choosing $\hat{n}_3 = 3n_3$ would be a suitable choice in our experiments.

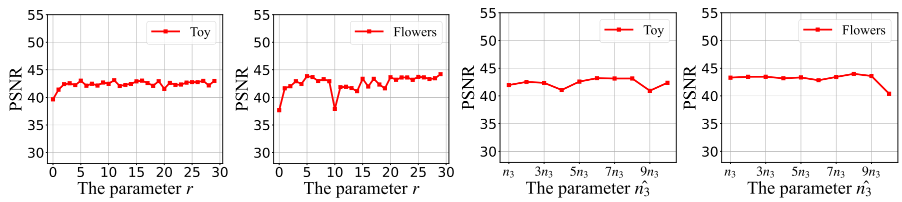

Fig. 2: The PSNR curves with respect to the parameter r and $\hat{n}_3$ for various data.

B.4 Role of the Layer Number of the MLP

We conduct experiments to evaluate the effect of the layer number of MLP ($i.e.$, l) on the performance of the proposed FLRTF. Fig. 3 illustrates the PSNR values corresponding to different l on MBI task. From Fig. 3, we can observe that when l is between 1 and 5, the PSNR value increases rapidly with the increase of l. The proposed FLRTF exhibits better performance when $l = 5$, and are stable as the number of layers increases. Based on this observation, we conclude that selecting $l = 5$ would be a suitable choice in our experiments.

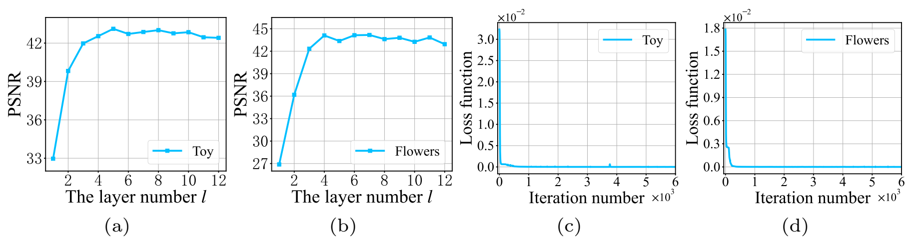

Fig. 3: (a)-(b): Performance with different layer numbers of MLP for various data. (c)-(d): The objective function values with respect to the iteration number for various data.

B.5 Convergence Behavior

We empirically demonstrate the convergence of the Adam-based solving algorithm of the proposed FLRTF, through numerical demonstrations. In Fig. 3, we present the evolution of training loss curves with respect to the iteration number on MBI task. Remarkably, our observations consistently demonstrate a steady decrease in training loss as the number of iterations increases. This observation proves the numerical stability and convergence of the proposed algorithm.

C More Experimental Results

Please see Figs. 4–5 for more visual results.

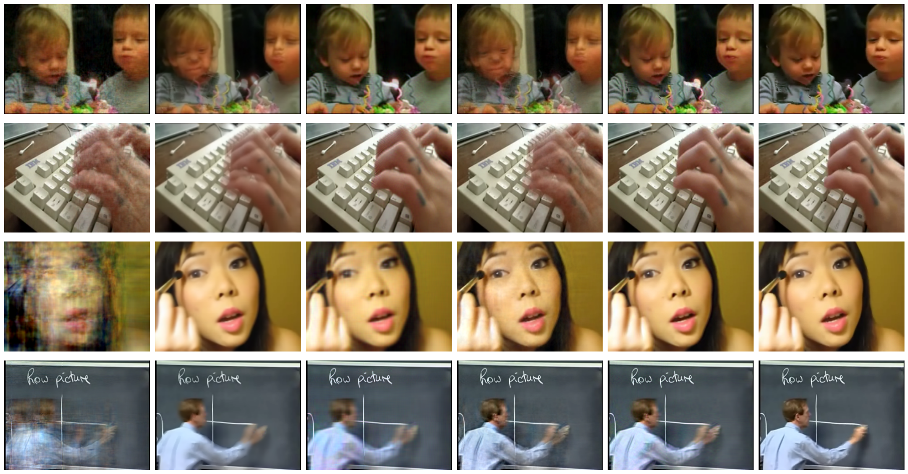

DCTNN TNN-3DTV HLRTF t-CTV FLRTF GT

Fig. 4: Visualization of recovery results by different methods for video frame extrapolation and interpolation tasks. From top to bottom: the 31 frame of *Blowing Candles*, the 31 frame of *Typing*, the 12 frame of *Apply Eye Make-up*, and the 28 frame of *Writing On Board*.

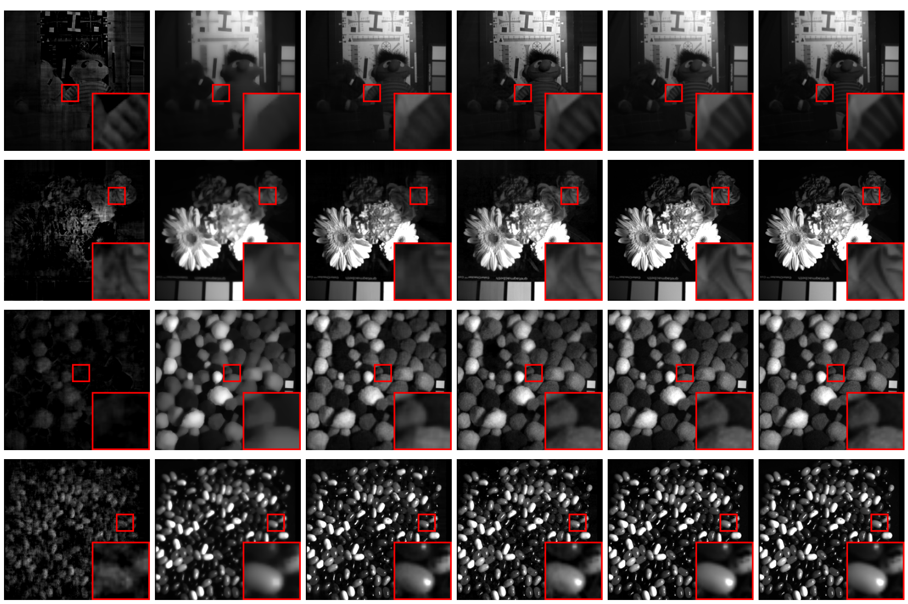

DCTNN TNN-3DTV HLRTF t-CTV FLRTF GT

Fig. 5: Visualization of the restoration results by different methods for MSI band interpolation task. From top to bottom: the 2 band of *Toy*, the 27 band of *Flowers*, the 15 band of *Pompoms*, and the 12 band of *Jelly Beans*.

References

1. Luo, Y., Zhao, X., Meng, D., Jiang, T.: HLRTF: Hierarchical low-rank tensor factorization for inverse problems in multi-dimensional imaging. In: 2022 IEEE/CVF Conference on Computer Vision and Pattern Recognition (CVPR). pp. 19281–19290 (2022)